Spatiotemporal characteristics and prediction of ecological safety in the Yellow River Basin of China

Xiao Wei, Lifeng Zhang*, Yi He**, Binhai Gao , Sheng Yao , Yujie Ding, Yan Guo, Ling Ran

***Abstracts*-The Yellow River Basin (YRB) is a major ecological functional area in China, and its ecological safety development and change have extremely significant impacts on the natural environment and human society. However, existing studies on the YRB lack spatiotemporal characteristics analysis and prediction of ecological safety with vegetation as the core. Therefore, this study proposes to construct an ecological safety index (ESI) of the YRB based on the comprehensive multi-dimensional ecological safety evaluation system "vigor-pressure-state-response," using the normalized difference vegetation index, vegetation carbon sink indicator parameters, temperature, precipitation, the digital elevation model, population density, and the per capita gross domestic product from 2000 to 2020. The spatiotemporal characteristics of the ESI were then analyzed for the YRB, and a long-term and short-term memory network model was constructed to predict the ESI trend of the YRB over the next 10 years. According to the results, from 2000 to 2020, the ESI of the YRB showed a fluctuating upward trend, and the annual average of the ESI changed abruptly in 2015 due to drastic changes in hazardous areas. The ESI in most areas of the YRB showed a significant upward trend, the stability of ESI changes was weak in some areas, and the overall spatial distribution showed significant positive spatial agglomeration characteristics. Further, the response of ESI to landscape complexity in different reaches of the YRB varied. Most of the middle reaches were positively correlated with landscape complexity, while most of the upper and lower reaches were not significantly or negatively correlated. Notably, over the next 10 years, YRB's ESI growth will slow down, with areas with degradation increasing, areas with significant growth decreasing, and areas currently showing stability improving.**

***Index Terms*—Yellow River Basin; ecological safety; evaluation system; LSTM; landscape indices**

This research was funded by the National Natural Foundation of China (Grants Nos. 42211530453), National Natural Science Foundation of China (Grants Nos. 42161063), and Key R&D Plan of Gansu Provincial Department of Science and Technology (23YFFA0057).(Corresponding authors: Lifeng Zhang; Yi He.)

Xiao Wei, Lifeng Zhang, Yi He, Binhai Gao , Sheng Yao , Yujie Ding, Yan Guo, Ling Ran, are with the Faculty of Geomatics, Lanzhou Jiaotong University, Lanzhou 730700, China, with the National-Local Joint Engineering Research Center of Technologies and Applications for National Geographic State Monitoring, Lanzhou 730700, China, and also with the Gansu Provincial Engineering Laboratory for National Geographic State Monitoring, Lanzhou730700, China (e-mail: 119273207@qq.com; heyi@mail.lzjtu.cn;2326779879@qq.com)

I. INRODUCTION

Ecological safety is a complex issue involving many aspects of nature, the economy, and society. It represents the overall integrity and health of the ecosystem. It is essential for protecting ecosystem stability, preventing environmental disasters, achieving sustainable development, and promoting human health and well-being [1]. Due to the extremely complex aspects of ecological safety and the many influencing factors, the intensity, duration, and spatial scope of ecological safety are often quantified by constructing an ecological safety index (ESI) [2]-[5]. The composite index method is widely used in ecological safety evaluations. The focus of this method is on constructing a standard index system to characterize ecological safety [6]. Currently, the more commonly used index system for evaluating ecological safety is the comprehensive multi-dimensional ecological safety evaluation system based on the "pressure-state-response" (PSR) framework. PSR is centered on the "state" dimension, which represents the environmental characteristics of an ecosystem. The "pressure" dimension reflects the impact of many elements of damage to the natural environment. Social and natural manifestations make up the "response" dimension [7]. However, due to the differences and characteristics of the study areas, there have been other multi-dimensional index systems similar to PSR. These frameworks generally include dimensions such as climate, natural environment, social, and economic conditions, and other factors [8].

The Yellow River Basin (YRB) is a crucial component of China's ecological safety and is an essential ecological functional area in China [9],[10]. However, the ecological safety of the YRB also faces many challenges. First, due to the complex terrain, there are abundant geomorphological types in the region, which leads to the diversity of land use and vegetation distribution and increases the vulnerability of the ecosystem. Second, the spatial distribution of temperature and precipitation is obviously unbalanced, and the difference between the east, west, south, and north is obvious, which poses a challenge to vegetation growth and water resource allocation [11]. Furthermore, social factors, such as continued population growth, accelerated industrialization, and urbanization, have led to the overexploitation and pollution of water resources, making ecosystems more fragile [12]. All these factors have intensified the ecological safety problems in the YRB, restricting the sustainable development of the natural environment and economic society in the region [13]. Therefore, given the urgent need to formulate an ecological

protection strategy for the YRB, it is necessary to analyze and predict changes in ecological safety within the YRB. This has important practical significance for improving the local ecological environment and coordinating the contradiction between economic development and the ecological environment protection of the region.

Vegetation, as the material base in the ecosystem of the YRB, plays an important role in the cycling of carbon, nitrogen, and other nutrients. It also has an irreplaceable role in climate regulation, soil conservation, and air improvement [14]. Thus, constructing an ESI with vegetation as the core can better capture the dynamic characteristics of the ecosystem in the YRB and clarify the trend of ecosystem change. However, most existing studies have evaluated the ecological safety of the YRB in recent years in terms of land cover changes or the identification of ecological protection zones [15]-[17]. These studies are slightly insufficient to consider the integrated ecological safety problems of the natural environment and human society in the YRB, as they neglect the holistic and systematic characteristics of the ecosystem of the YRB. Further, only a few studies have constructed an ESI of the YRB, and their evaluation index systems are confusing, failing to verify the validity of the constructed index system and the ESI and lacking logical and dynamic features [18],[19]. In addition, these studies mainly focus on the retrospective evaluation of ecological safety, lacking research on ecological safety prediction and early warning.

Therefore, this study adds vegetation as the "vigor" dimension to the core of the comprehensive, multi-dimensional ecological safety evaluation system, "vigor-pressure-state-response," which includes natural geographical conditions, climatic conditions, and human activities, to construct an ESI of the YRB and predict the future development trend of the YRB's ESI. The study uses data from the normalized difference vegetation index (NDVI), gross primary productivity (GPP), temperature, precipitation, digital elevation model (DEM), population density, and per capita gross domestic product (GDP) in the YRB from 2000 to 2020. We explore the spatiotemporal variation characteristics of YRB's ESI and the relationship between the ESI and different landscape indices in the process of change for the past 20 years through statistical analysis. Lastly, we use the long-term and short-term memory network (LSTM) to predict the ESI changes in the YRB based on the existing change characteristics and analyzed the trend of the prediction results. Our findings provide data and theoretical support for ecological environment construction and sustainable economic development in the YRB.

II. OVERVIEW OF THE STUDY AREA

The YRB originates from the northern foothills of the Ba Yan Ka La Mountains on the Qinghai-Tibet Plateau, and flows through Qinghai, Sichuan, Gansu, Ningxia, Inner Mongolia Autonomous Region, Shanxi, Shanxi, Henan, and Shandong, with a watershed area of 794,600 km^2, as shown in **Fig. 1**.

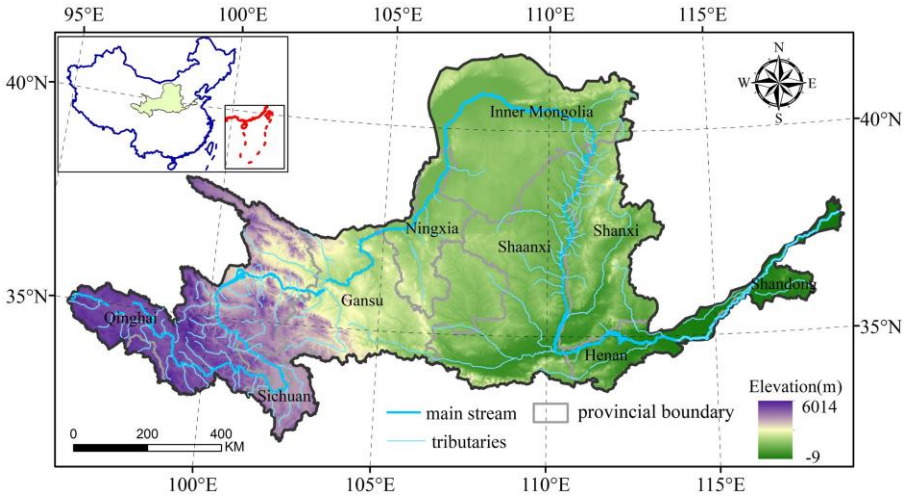

Fig. 1 Geographic location of the YRB

The terrain of the YRB gradually declines from west to east, with an average elevation of more than 4000m in the western region, mostly high-altitude mountains; the central region, with mostly high-altitude mountains. The central region has an elevation of 1000–2000m and is dominated by loess landforms. The eastern region, with an elevation of no more than 100m, is mainly constituted by the YRB impact plains [20]. The YRB covers three distinct climatic zones in the east, center and west, with semi-humid, semi-arid and arid climates, respectively. This leads to the obvious geographical distribution difference of annual precipitation in the YRB. The source area is located in the Qinghai-Tibet Plateau, and the annual precipitation is low, generally between 200-400 mm. In the middle reaches of the basin, especially through Shaanxi and Inner Mongolia, the annual precipitation is also relatively low, about 400-600mm. In the lower reaches, especially in Shandong Province near the estuary, the annual precipitation can increase to more than 800 mm. The temperature distribution in the YRB also shows significant geographical characteristics. The annual average temperature of the Tibetan Plateau in the source area of the basin is low, especially cold in winter and cool in summer. In the middle

reaches, including Shaanxi and Inner Mongolia, the annual average temperature is relatively mild, but it is cold in winter and warm in summer. The downstream area is affected by the ocean, and the climate is relatively mild, warm in winter and cool in summer. Against the backdrop of complex topography and climate, the YRB is likewise confronted with the various impacts of resource depletion, pollution, land degradation and climate change. These problems affect agriculture, ecosystems and human societies, and their ecological safety is becoming more and more prominent.

III. DATA SOURCES AND RESEARCH METHODS

This study analyzed the ESI changes and development of the YRB in three parts (**Fig. 2**). The ESI was constructed based on a comprehensive, multi-dimensional ecological safety evaluation system. The spatiotemporal variation characteristics of YRB's ESI from 2000 to 2020 were then explored. The relationship between ESI and the landscape index was analyzed. Lastly, the spatial distribution of the ESI over the next 10 years was predicted, and the spatiotemporal characteristics were analyzed.

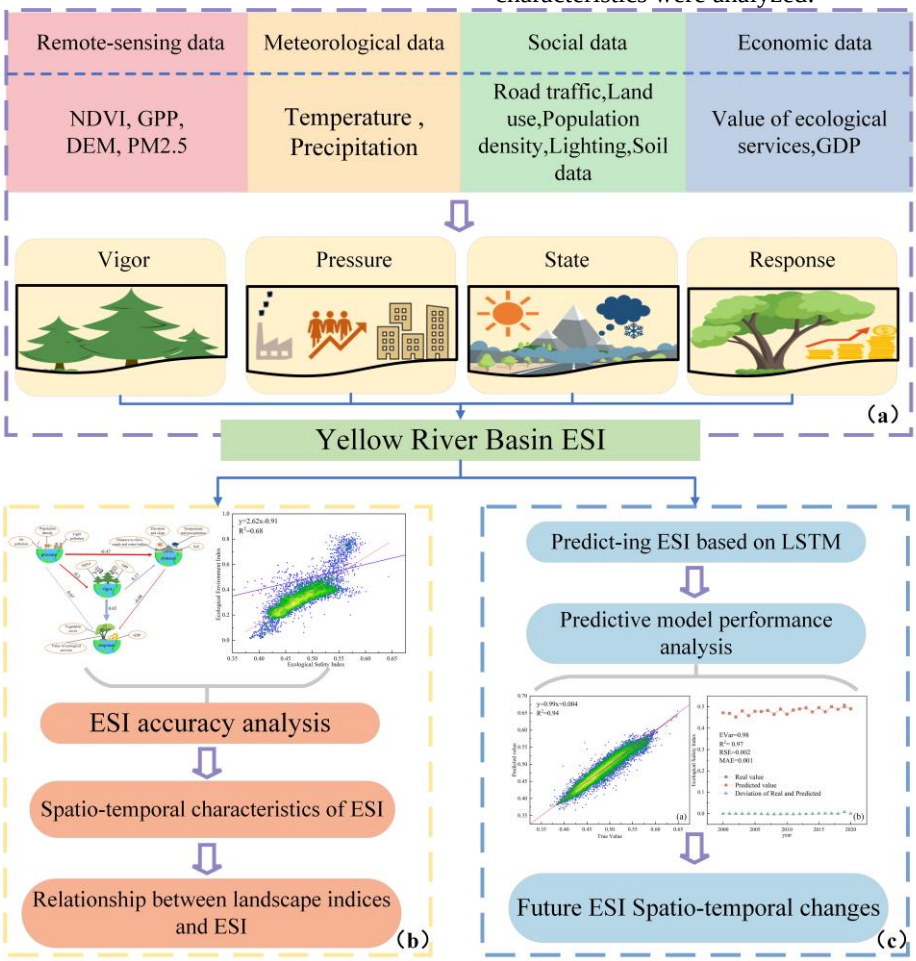

Fig. 2. Flow chart of the study

A.Data sources and processing

The basic data used in this paper include remote sensing data, NDVI, GPP, DEM, road traffic data, GDP data, temperature, precipitation data, population density data, and the Eco-Environmental Quality Index (EQI). The sources, descriptions, and uses of the relevant data are described in detail in **Table 1**. To unify the accuracy, taking into account the characteristics of the basic data and the computability, all the data were resampled at 1000 m×1000 m. Each data set used is described in detail in **Table 2**.

Table 1

Data types and sources

Data name	Data time	Data accuracy	Data sources
NDVI	2000-2020	1000m	https://lpd-aac.usgs.gov//
GPP	2000-2020	0.05°	http://globalecology.unh.edu/data/GOSIF.html
Road traffic	1995-2020	-	http://www.resdc.cn/

DEM	--	30m	http://srtm.csi.cgiar.org//
Land use	2000-2020	1000m	http://www.resdc.cn/
Temperature and precipitation	2000-2020	1000m	http://loess.geodata.cn/
PM2.5	2000-2020	0.01°	https://sites.wustl.edu/acag/datasets/surface-pm2-5/#V5.GL.02
Population density	2000-2020	30arcsecond	https://www.worldpop.org/
Lighting	2000-2020	15arcsecond	https://doi.org/10.7910/DVN/YGIVCD
GDP	2000-2020	1000m	http://www.resdc.cn/
Value of ecological services	2000-2020	1000m	https://doi.org/10.7515/JEE222022
Soil	1995	1000m	http://www.resdc.cn/
Eco-Environmental Quality Index	2000-2020	500m	https://lpdaac.usgs.gov/products/mod09a1v006/

B.Research Methods

1)Construction of ESI

The ecosystem of the YRB is composed of multi-attribute and multi-level subsystems. Therefore, we build an ecological safety evaluation system and combined with the characteristics of natural environment and social economy in the study area. In the construction of ESI system, the vegetation as the core reflects the deep understanding of the regional ecosystem function and ecological service value. The deep-seated reasons for this approach include plant support for biodiversity, carbon fixation and oxygen production, regulation of hydrological cycle and soil protection [21]. The potential advantages are mainly that it emphasizes the comprehensive assessment of ecosystem versatility and the use of vegetation sensitivity to track ecosystem changes [22]. Compared with the traditional ecological safety assessment methods, the multi-dimensional and multi-index evaluation system with vegetation as the core can provide more timely feedback and early warning for ecological safety changes. Further, this approach yields an ESI system with better adaptability and flexibility, one that can be adjusted and optimized according to the characteristics of different ecosystems and the impact of human activities. The specific construction process of the evaluation system is shown in **Fig. 3**.

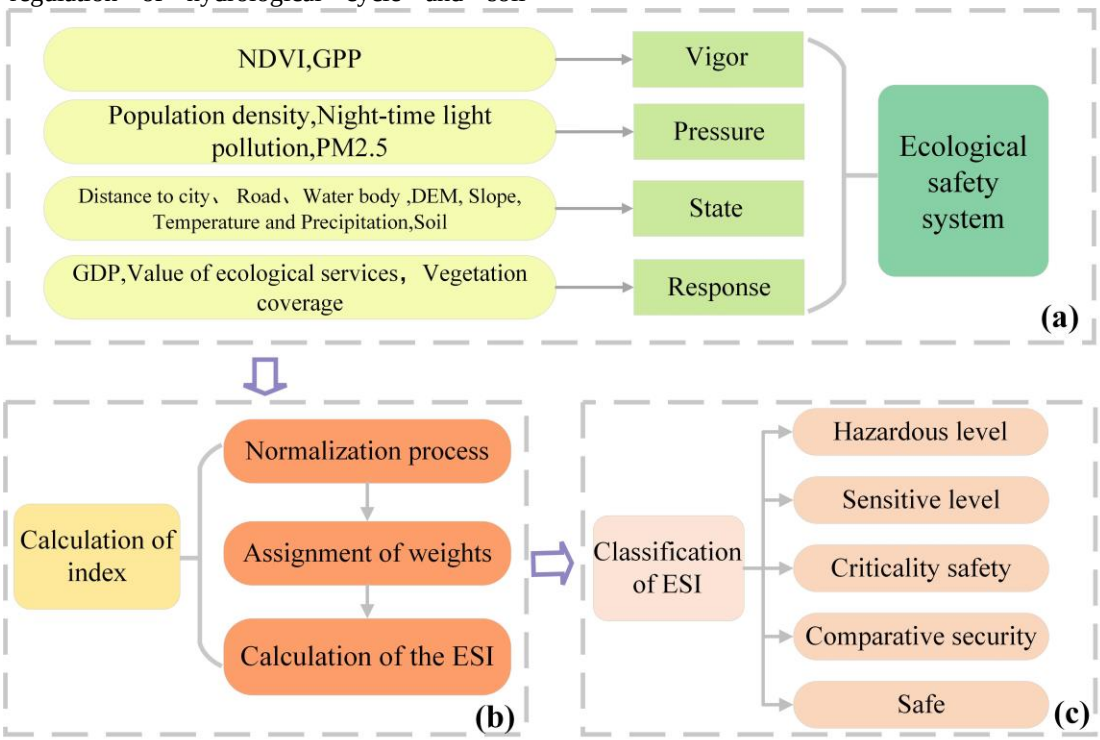

Fig. 3.Flow chart of the construction of the ESI of the YRB

a) Ecological safety system

Vigor is the productivity and metabolic capacity of a regional complex ecosystem to maintain its sustainability [23]. Therefore, we construct the vigor index layer as the basis of the energy cycle in the ecological environment. Vegetation, as a major factor in the vitality of ecosystem, is not only important in providing food and energy and maintaining biodiversity but also participates in the regulation of the water cycle and soil protection, and plays an important role in climate regulation [24]. Therefore, maintaining the ecological function of vegetation is essential for the stability of the ecosystem and the sustainable development of human beings. NDVI as an indicator of vegetation growth state, the greater its value, the denser vegetation cover, the more conducive to the stability of the ecosystem [25],[26]. GPP refers to the overall quantity of carbon sequestered by a terrestrial ecosystem through the process of vegetation photosynthesis. It serves as the initiation point of the carbon cycle and serves as an indicator of the productivity level within terrestrial ecosystems [27],[28]. Therefore, we selected two indices, NDVI and GPP, to represent vegetation as an index of the vigour injected into the ecosystem.

Pressure is a direct factor in the ecological burden. The pressure in the YRB mainly comes from a series of human activities in the ecosystem. High population density is usually accompanied by a large number of urbanizations, land development, and infrastructure construction, which leads to the destruction of the habitat of the ecosystem. A high population density increases the pressure to consume resources, further exacerbating the impact on the ecosystem [29]. Light pollution has also become a major threat to the destruction of ecology with the intensification of human activities. This is usually caused by excessive floodlight and artificial light generated by city night lighting. It destroys the biological clock and circadian rhythm and has great harm to the ecosystem [30]. PM2.5, an indicator of industrial pollution, is released in large quantities from industrial activities and can interfere with the photosynthesis of plant leaves and reduce plant growth and yield. PM2.5 also promotes soil acidification and water pollution, which are detrimental to the soil quality of the ecosystem and the ecology of water bodies [31],[32]. Therefore, we selected population density, light pollution, and PM2.5 pollution as three typical factors in the main index of pressure.

State of the region is a realistic representation of the ecosystem. Geographical and climatic environments are the main factors that make up the state, and they directly influence the stability of the ecosystem [33]. Here, we used distance from cities, transportation roads, water bodies, soil, DEM, and slopes as the topographical state of the ecosystem. According to existing studies, we found that the upward trend of vegetation decreases with increasing altitude and slope in the YRB. Meanwhile, temperature, and precipitation promote vegetation growth in the YRB as a whole, and the stronger the stability of the soil, the more stable the vegetation growth state [34]. Based on the influence trend of these factors on vegetation growth, we assessed the relationship between the ESI of the YRB and these influencing factors to construct the corresponding state.

Response is the social and natural reflection of the ecological environment on vigor, pressure, and state. ESI needs to comprehensively consider the relationship between nature and human activities, so we chose GDP as a social response. The growth of GDP can increase investment in environmental protection, promote green technology innovation, and raise awareness of ecological protection, thus promoting ESI [35].Vegetation coverage reflects the health and sustainability of ecosystems as a natural response [36]. The value of ecological services is calculated through the input of natural data and economic methods as a common response between society and nature [37]. Therefore, we combined the characteristics of these three indices to construct the response.

b) Calculation of index

In the process of ecological safety assessment, the initial data should be standardized to eliminate inconsistency between size and value, which has a great impact on the results. In general, all indicators of ecological safety evaluation can be divided into negative indicators and positive indicators. The larger the positive indicators, the better the evaluation object [38]. The normalization method is as follows:

$$Y = \frac{x - x_{min}}{x_{max} - x_{min}} \quad (1)$$

The smaller the negative indicators, the better the evaluation object. The normalization method is as follows：

$$Y = 1 - \frac{x - x_{min}}{x_{max} - x_{min}} \quad (2)$$

where X_{max} is the maximum value of variable X; X_{min} is the minimum value of variable X, and Y is the normalized variable value.

This study adopted the entropy weight method to solve indicator weights. The entropy weight method is an objective weighting method that assigns weights to indicators by comparing the information differences between indicators. This method has widespread application in multi-indicator evaluation systems, as it adeptly mitigates the impact of human factors on weight assignments [39]. Its specific calculation steps are as follows:

Calculate the information entropy of the *j*th indicator:

$$E_j = -\ln(n)^{-1} \sum_{i=1}^{n} P_{ij} \ln P_{ij} \quad (3)$$

where $P_{ij} = Y_{ij} \Big/ \sum_{i=1}^{n} Y_{ij}$, $Y_{ij}$is the value of the normalized indicator.

Calculate the weight of the jth indicator:

$$W_j = \frac{1 - E_j}{k - \sum E_j} \quad (4)$$

Calculation of the ESI：

The final ESI is determined by weighting

$$Z = \sum_{i=1}^{k} X_{ij} \cdot W_j \quad (5)$$

Table 2

Evaluation index system of ecological safety in the YRB

Target level	Criterion layer	Index layer	Safety trend	Weights
Comprehensive evaluation index of ecological safety	Vigor (weights0.2636)	NDVI	+	0.4590
		GPP	+	0.5410
	State (weights0.2411)	Distance to cities	+	0.2070
		Distance to roads	+	0.2204
		Distance to water bodies	-	0.1940
		DEM	-	0.1855
		Slope	-	0.1932
		Precipitation	+	0.3654
		Temperature	+	0.3050
		Soil	+	0.3296
	Pressure (weights0.2393)	Population density	-	0.3312
		PM2.5	-	0.3375
		Lighting	-	0.3313
	Response（weights0.256）	GDP	+	0.3436
		Value of ecological services	+	0.3249
		Vegetation coverage	+	0.3315

c) Classification of ESI

In this study, by referring to the results of previous studies and the basis of ecological safety evaluation in the region, the ESI artificially sets breakpoints [40],[41].We divided ESI into type I hazardous level, type II sensitive level, type III critical safety level, type IV comparative safety level, and type V safety level. Specific descriptions are shown in **Table 3**.

Table 3

ESI classification table of the YRB

ESI	Safety level	Safety state	Description
0.3-0.44	I	hazardous	Ecological safety has been damaged to such an extent that it is difficult to recover, and the ecological environment is incomplete and dysfunctional, making it difficult to meet the development needs of the ecosystem.
0.44-0.47	II	sensitive	Ecological safety has been more seriously damaged, ecological sensitive is high, ecological functions are seriously degraded, and ecological pressure is higher.

0.47-0.5	III	critical safety	Ecological safety is affected to some extent, ecological structure is intact but there are some ecological anomalies and some ecological pressure
0.5-0.53	IV	comparative safety	Ecological safety has been slightly damaged, and the system is more resilient. The land ecosystem is relatively well structured and can withstand most external disturbances. It can be restored to a healthy state.
0.53-0.7	V	safety	Ecological safety is virtually unaffected and overall ecological functioning is sound. The ecological structure is intact and the ecosystems in the region are sustainable.

2)Calculation of landscape indices

We categorized six land types—grassland, woodland, urban, and rural construction land, wetland, arable land, and unvegetated areas—according to the current land use status in the study area. We utilized these categories to compute four landscape indices [42],[43]: cohesion, patch density (PD), Shannon's diversity index (SHDI), and landscape shape index (LSI). These four landscape indices can comprehensively reflect the structural and functional characteristics of the landscape from different perspectives. Each indicator focuses on a unique aspect of the landscape and together provides a comprehensive description of landscape complexity. Further, these indexes are interrelated and influence each other. The formulas and ecological significance of each landscape index are presented in **Table 4.**

Table 4

Landscape indices calculation formula and ecological significance

Landscape Index	Calculation formula	Ecological significance
Cohesion	$COHESION = \left[1 - \frac{\sum_{j=1}^{m} p_{ij}}{\sum_{j=1}^{m} p_{ij}\sqrt{a_{ij}}}\left[1 - \frac{1}{\sqrt{A}}\right]^{-1}\right] \times 100$	Cohesion is often used to measure the degree of connection between units in a landscape. where a_{ij} refers to the area of the j-th patch in the i-th landscape; p_{ij} represents the perimeter of the j-th patch in the i-th landscape; and A is the total area of the landscape.
PD	$PD = \frac{N}{A}$	PD responds to the degree of fragmentation of the landscape, with larger values indicating greater fragmentation of the landscape, where N is the total number of all patches in the landscape and A is the total area.
SHDI	$SHDI = -\sum_{i=1}^{m}(p_i)\log_2 p_i$	SHDI reflects the richness and evenness of species within the landscape, with larger values indicating species with richness and balanced richness among each other, where P_i is the proportion of patches of landscape type i to all patches in the landscape.
LSI	$LSI = \frac{0.25E}{\sqrt{A}}$	The smaller the LSI value, the more regular the shape of the landscape; the larger the LSI value, the more complex the shape of the landscape tends to be, where A is the total area, E is the total length of all patch boundaries in the landscape, and 0.25 is the square correction factor.

3)Statistical analysis

a) Mann-Kendall mutation test

In this study, we used the Mann-Kendall (MK) mutation test to further explore the temporal variation characteristics of the ESI. The MK test is a non-parametric statistical method endorsed by the World Meteorological Organization and enjoys extensive application. Its advantages are that it does not need to assume that the samples follow a particular distribution and that it is not susceptible to individual outliers. The method has a high degree of quantification, a wide range of detection, and ease of computation. Therefore, it is more suitable for the analysis of ordinal and typological variables [44]. The trend of the time series is determined by calculating two statistical variables UFk and UBk. In the test curve, if the UFk line in the test curve changes within the critical line. We observed that the trends and mutations in the change curve were not distinctly evident. A UFk value greater than zero indicates that the sequence is on the rise, less than zero indicates a downward trend, and a value that exceeds the critical line indicates that the upward or downward trend is significant. If the two curves of UFk and UBk intersect between the critical lines, the moment corresponding to the intersection is the time when the mutation begins. If the intersection point appears outside the critical line, or there are multiple intersections, the method can be combined with other test methods to further determine whether it is a mutation point.

b) Spatial autocorrelation analysis

We used spatial autocorrelation analysis to explore the spatial distribution of the ESI. The Moran's index (Moran's I) is a common method for assessing the spatial autocorrelation of various indicators, which can be divided into two forms: global Moran's I and local indicators of spatial autocorrelation (LISA). Moran's I is used to indicate the clustering trend across the region, with negative values indicating negative spatial correlation and positive values indicating positive spatial correlation, and the magnitude of the value reflecting the strength of spatial autocorrelation [45]. LISA can further reflect the high- and low-value agglomeration characteristics of positive and negative local spatial autocorrelation according to the four types of spatial correlation between a given location and its neighbors. These are the spatial characteristics of high–high agglomeration, low–low agglomeration, high–low agglomeration, and low–high agglomeration. In this paper, we used GeoDa software to calculate the Moran's I and LISA of YRB's ESI to explore its spatial distribution characteristics.

c) Trend analysis

We used Theil-Sen (TS) trend analysis and Mann-Kendall (MK) significance tests to explore the spatial variation characteristics of ESI. The TS and MK are reliable nonparametric statistical trend analysis methods, and TS provides more accurate results compared to simple linear regression[46],[47]. The calculation principle of TS is to divide the time series data into n(n-1)/2 pairs of combinations, and then calculate the slope β of the median value of each data pair. If $\beta > 0$, it indicates an upward trend change; if $\beta < 0$, it indicates a downward trend change. MK is a nonparametric test for examining the trend of a time series, which has the advantage of eliminating the need to suppose that the data follow a particular distribution and allowing for the presence of missing values. The MK statistic U takes values from $-\infty$ to $+\infty$. If $U > 0$, the time series has an upward tendency; if $U < 0$, the time series has a downward trend. When |U| is less than 1.96, the trend changes significantly($p<0.05$).

d) Stability analysis

To explore the spatial variation characteristics of ESI, we used the coefficient of variation (CV) to evaluate the stability of ESI [48]. The formula can be written as follows:

$$CV = \sigma/\mu \tag{6}$$

$$\sigma = \sqrt{\frac{1}{N}\sum_{i=1}^{N}(x_i - \mu)^2} \tag{7}$$

$$\mu = \frac{1}{N}\sum_{i=1}^{N} x_i \tag{8}$$

where σ is the standard deviation of the annual ESI; μ denotes the mean value of the ESI; N represents the number of years in the study period; and x_i represents the value of the ESI in the year i.

e) Correlation analysis

We used Pearson's correlation analysis to explore the relationship between ESI and the landscape index. Pearson correlation analysis is a commonly used statistical analysis method for measuring the degree of linear correlation between two variables [49],[50]. It calculates the correlation coefficient r between variables based on the concept of covariance. The interval of r is [-1,1], when $r < 0$ means that the two are negatively correlated; $r > 0$, positively correlated; $r = 0$, no correlation.

f) Structural equation modeling(SEM)

We used SEM to validate the rationality of ESI construction. SEM is a multivariate statistical method that uses linear equations to express the relationships between observed and latent variables. As a validation model, SEM combines factor analysis and path analysis, enabling the description of intricate multivariate statistical relationships among variables that are not directly measurable[51],[52]. There are two kinds of variables in the SEM, one is a measurable explicit variable, and the other is a latent variable that cannot be directly measured. SEM comprises two integral components: the measurement equation and the structural equation. The measurement equation elucidates the association between latent variables and observed variables, and the structural equation delineates the connections among latent variables themselves.

4)Spatiotemporal prediction model

The LSTM network is a specific recurrent neural network (RNN) architecture that excels in time-series prediction. It learns potential patterns and trends in time-series data that can be utilized to predict future values and changes [53],[54]. In this paper, based on the 2000-2020 time series ESI data, a spatiotemporal prediction model of ecological safety was constructed based on an LSTM neural network. The specific process is as follows:

Data preparation: Initially, time series images spanning 2000 to 2020 were read and amalgamated into a matrix, with the time dimension designated as the third dimension. Subsequently, effective pixels were extracted and differentially processed. Considering potential blank pixels due to surrounding areas or river changes at certain time steps, the extraction criterion was that the time series would be completely non-empty.

Dataset segmentation: In alignment with the prediction model design, the dataset was segmented for each pixel time series based on the input time step. As the prediction model involved a many-to-many output, multiple time steps were employed to predict a single time step. Subsequently, a sliding window was employed to section the dataset, where the window width equaled the length of the input time step, and the step size was set to 1. The last five datasets served as test sets, while the remaining data were partitioned into training and validation sets at a ratio of 4:1.

Model construction and training: The model devised in this study adopted a linear encoder-predictor-decoder framework. **Fig. 4** illustrates the model structure and setup. For model training, an Adam optimizer and Logcosh loss function were employed. The training cycle (epoch) was set at 128, with each epoch comprising 64 steps. The batch size was set to 512, and the initial learning rate was fixed at 0.0001.

Model prediction applications: The trained model was applied to predict each effective pixel, and the predicted difference sequence data were augmented with the initial value to derive the predicted sequence. Subsequently, the prediction sequence of the effective pixel was stored in a

matrix corresponding to the original pixel position. Lastly, the matrix was sliced along the time dimension and output as raster data for various time steps.

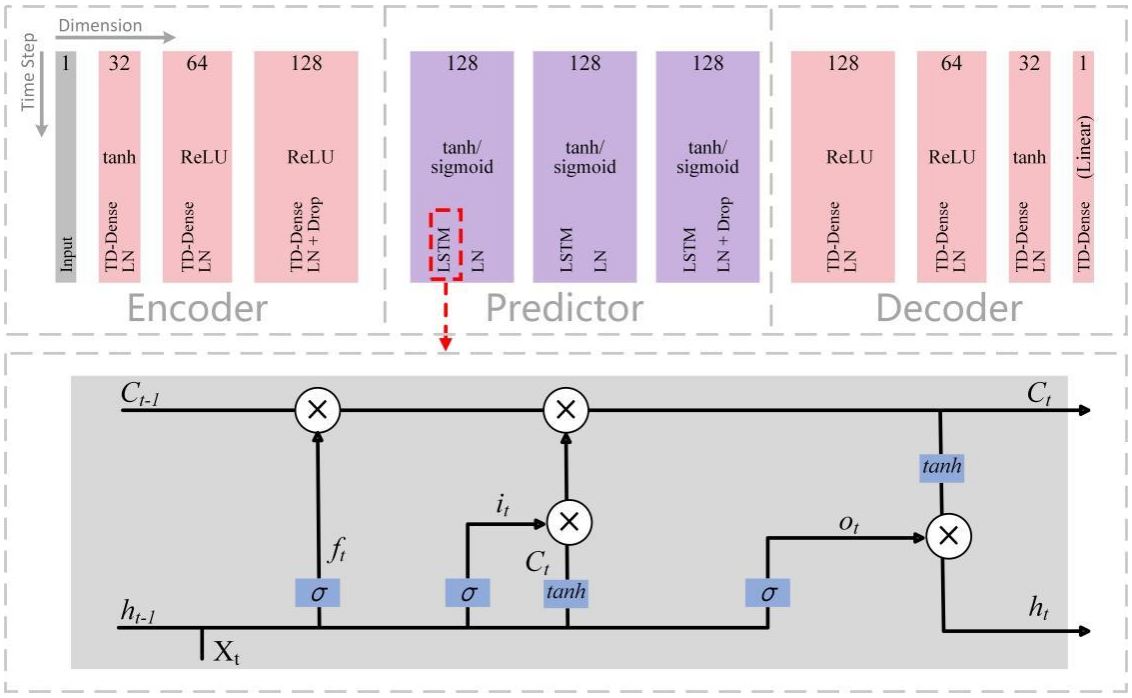

Fig. 4.Predictive model structure setup

IV. RESULT

A.Spatiotemporal characteristics of the YRB's ESI

1）Temporal change characteristics of the YRB's ESI

We linearly fitted the trend changes in ESI from 2000 to 2020 and explored the interannual variation characteristics of ecological safety in the YRB, as shown in **Fig. 5a**. From 2000 to 2020, the ESI of the YRB showed an upward trend, at a rate of 0.0016/a, indicating that the overall ESI has shown a good development state in the past 20 years. The change in the ESI index had obvious stage characteristics. The ESI showed a significant downward trend from 2000 to 2002, reaching the lowest value of 0.45 in 2002. There were also significant fluctuating changes from 2003-2016, and starting in 2016, the ESI showed a significant increase, reaching a maximum value of 0.51 in 2019. Combined with **Fig. 5b**, the ESI mutated in 2015.

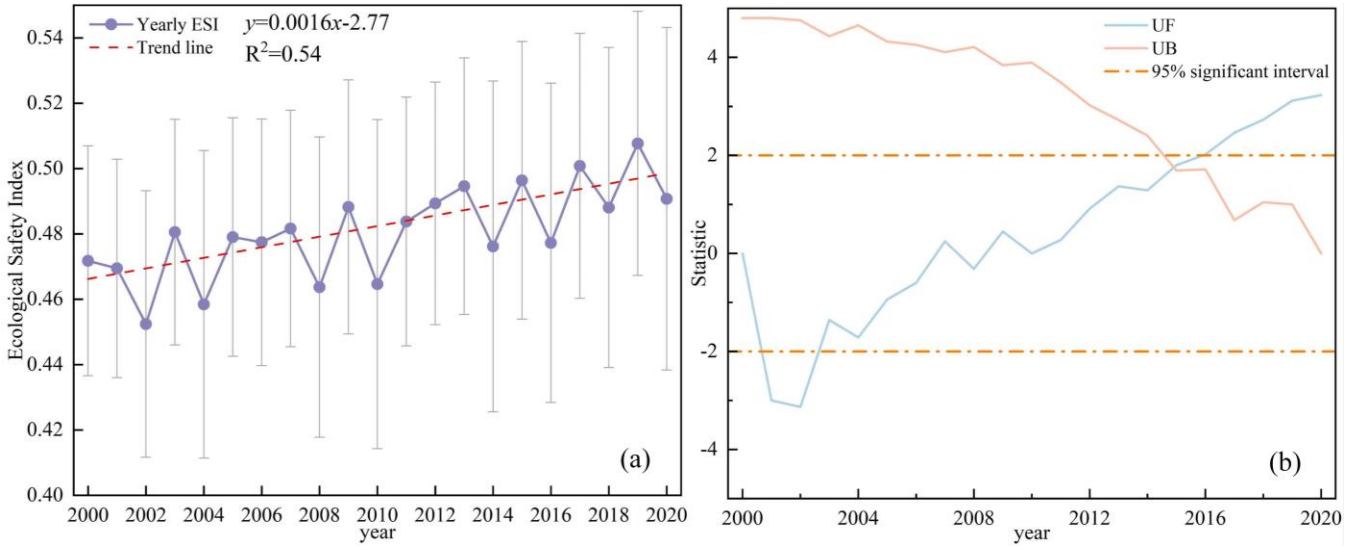

Fig. 5. Time-series changes of ESI in the YRB from 2000 to 2020 (a) mutation test (b)

For a deeper exploration of the reasons for the mutation in 2015, we visualized the area shift of the different levels of ESI in four time periods during the 2 years before and after the mutation point 2015 in the form of Sankey diagrams. As

shown in **Fig. 6**, from 2013 to 2014, the YRB showed a gradual shift in ESI from a good state to a bad state. Most of the sensitive areas were converted to hazardous levels. From 2014 to 2015, there was a cascading shift from bad to good ESI regions. The hazardous area was reduced in one large area, which was mainly transformed into a sensitive area and a critical safety area. Most of the sensitive areas became critical safety states, and the increase in the safety state area mainly came from the transfer of comparative safety and critical safety areas. The hazardous area increased during 2015-2016, with more than 50% of sensitive areas moving to hazardous areas. Some of the safe areas turned into comparative safe areas, and the overall trend of degradation appeared. There was a large reduction in hazardous areas during 2016-2017, with a major shift to sensitive areas and a corresponding increase in the size of safe areas. In summary, the main reason for the mutation of the annual average ESI in 2015 was the sharp decrease in the proportion of dangerous areas in 2014-2015 and the sharp increase in the proportion of hazardous areas in 2015-2016. In addition, different levels of ESI showed fluctuating step-by-step transfers. This shows that ESI improvement is a relatively slow time course and that changes are erratic, requiring control and governance over a long period of time.

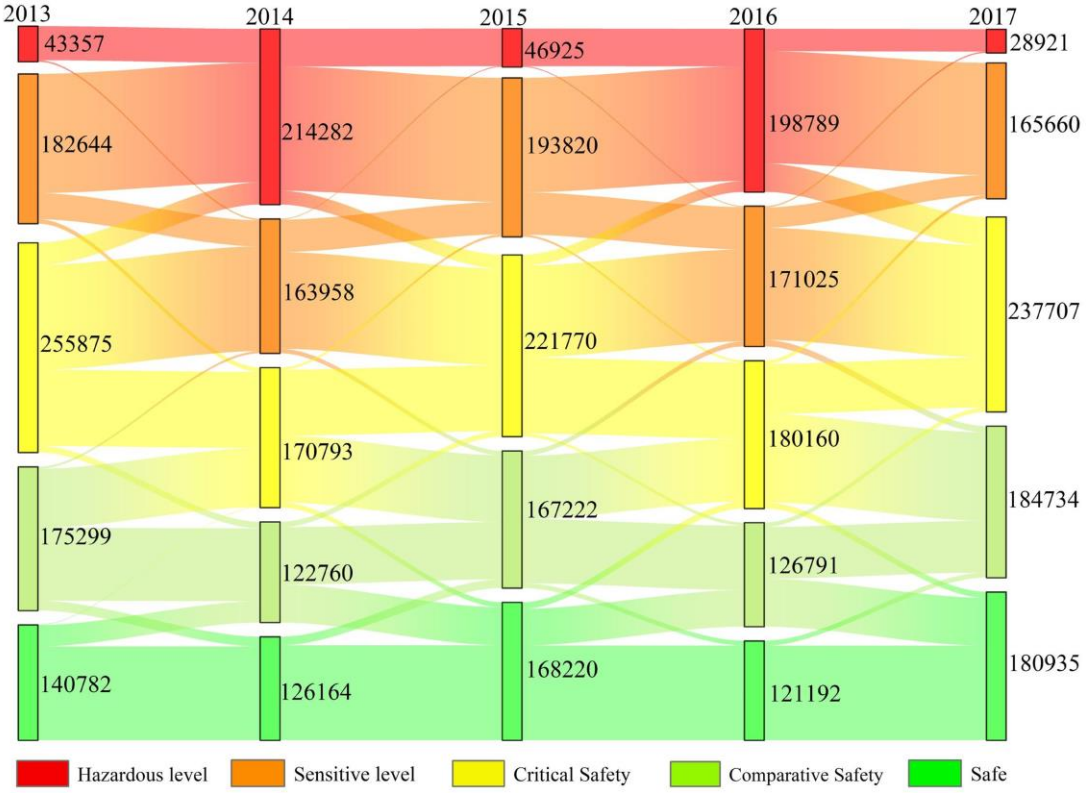

Fig. 6. Area transfer of ESI in the YRB, 2013-2017(km^2)

2) Spatial change characteristics of the YRB's ESI

The spatial distribution and proportion of different levels of the ESI in 2000-2020 are shown in **Fig. 7a**. We observed that the spatial distribution of the ESI was quite different in the YRB. For example, hazardous areas and sensitive areas accounted for 16.6% and 27.9%, respectively. They were mostly distributed in the upper reaches of the Hetao Plain, the Ordos Plateau, the Ningxia Plain, the western part of the Qinghai-Tibet Plateau, and the eastern part of the Loess Plateau. Most of the regions were mainly composed of arid and semi-arid regions, such as the Kurchi Desert and Maowusu sandy land. There was very little annual precipitation here, and it was affected by human activities, such as overgrazing and mining. This made the soil in these desert areas prone to desertification and loss of soil fertility and resulted in infertile vegetation, sparse species populations, loss of many ecological functions, and fragile ecosystems [55]. The ESI in a small number of urban areas with rapid development was also hazardous and sensitive, which was caused by a large number of land development and construction activities, pollutant emissions, and unreasonable land use in the process of urbanization. We observed a trend of gradual diffusion to their surroundings, and these diffusion areas showed critical safety levels. The proportions of safe areas and relatively safe areas were 12.7% and 18.4%, respectively. They were mainly distributed in the southwest and Qilian Mountains in the upper reaches and in the south and lower reaches in the middle reaches. The critical safety area accounted for 24.3%, which was mainly distributed between the safety area and the hazardous area as a buffer zone.

To elucidate the spatial distribution of ESI more distinctly, we conducted a spatial autocorrelation analysis on ungraded ESI. The Moran's I for ESI was 0.957, with a p-value below 0.05. **Fig. 7b** shows that the spatial agglomeration of YRB's ESI from 2000 to 2020 was mainly characterized by high-high aggregation and low-low aggregation, with an area ratio of 27.60% and 32.2%,

respectively, showing a continuous sheet distribution. The areas of high-low aggregation and low-high aggregation were very small, both of which were 0.04%, showing a scattered distribution, and the agglomeration effect was not obvious. Compared with agglomeration in **Fig. 7a**, the high-high aggregation mainly corresponded to the safe and relatively safe area, the low-low aggregation mainly corresponded to the hazardous area and sensitive area, and the non-significant area corresponded to the critical safe area, which further showed that our level setting was reasonable.

In summary, the ESI distribution showed obvious spatial differences in the YRB. Hazardous areas and sensitive areas were mainly concentrated in upstream and midstream urban areas. The critical safety area acted as a buffer area between low ecological safety and high ecological safety. The spatial autocorrelation analysis showed that the ESI exhibited significant positive spatial clustering characteristics in the YRB.

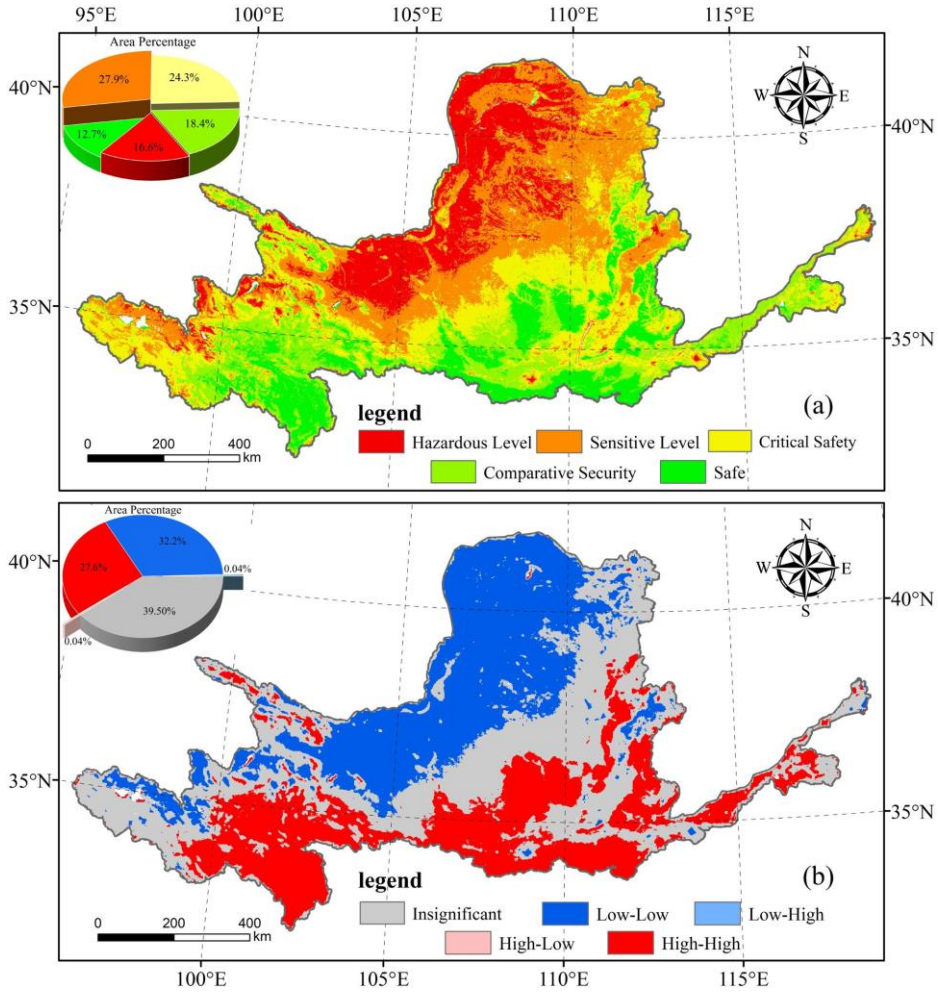

Fig. 7. (a) Spatial distribution of ESI in the YRB from 2000 to 2020; (b) Spatial autocorrelation of ESI in the YRB from 2000 to 2020

Based on the spatial distribution of the constructed ESI, we analyzed the spatial changes in the ESI of the YRB from 2000 to 2020, as shown in **Fig. 8a**. As shown in the diagram, the areas of significant improvement and slight improvement accounted for a large proportion, which were 71.9% and 21.7%, respectively. The desert arid area showed a good improvement trend in some parts of the northwest. The areas of severe degradation and slight degradation were very small, at only 0.2% and 0.4%, respectively. Most of them were urban areas with a high intensity of human activities. It was mainly distributed in Dongying (a), Tai'an (b), Zhengzhou and Luoyang (c), Taiyuan (d), Xi'an (e), Hohhot (f), Yinchuan (g), Lanzhou (h), and the northwestern part of Qilian Mountains (i). The downward trend of the ESI in the above area diverged from the city center to the surrounding area and gradually weakened. The stable and unchanged areas accounted for 5.8%. Their primary distribution was observed in the Hetao Plain, the Ordos Plateau, and the Ningxia Plain, as well as in regions where the divergence of the degradation trend weakened toward the surrounding area. Further, according to the coefficient of variation that we calculated, the stability of the ESI in the southwest region of the YBR was the best (**Fig. 8b**). The regions experiencing significant fluctuations were predominantly concentrated in the northwest region of the upper reaches, characterized by severe desertification, and in the more developed animal husbandry area in the western part of Sichuan Province. In summary, except for the slight improvement in the northwest region, ESI in most areas of the YRB showed a significant improvement trend. Degraded areas were primarily found in a limited number of urban areas characterized by intense human activity. Stability was weaker in regions with high

desertification, developed animal husbandry, and high ESI values on the Loess Plateau.

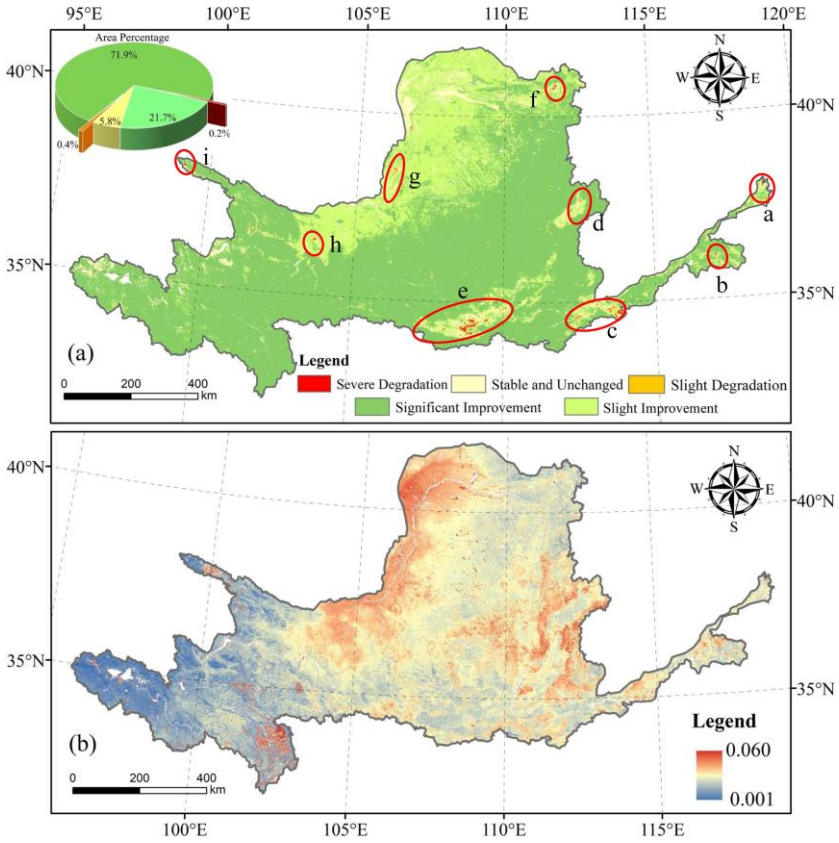

Fig. 8.(a) Spatial distribution of ESI trends in the YRB from 2000 to 2020; (b) Spatial distribution of ESI variation indices in the YRB from 2000 to 2020

B. Relationship between ESI and landscape indices

The spatiotemporal changes in ESI are closely related to the evolution of landscape indices. This is due to the change in landscape spatial structure, which will be reflected in the structural composition of the ecosystem, thus affecting the development and change of ESI [56],[57]. Therefore, we studied the correlation between ESI and cohesion, PD, SHDI, and LSI. Cohesion was positively correlated with the ESI over a large area in the eastern region of Qinghai Province in the upper YRB, as shown in **Fig. 9a**. This shows that the higher the spatial compactness and connectivity of the landscape in the region, the more conducive it is to improving the ESI. This suggests that the positive impact of connectivity in the region on ESI is reflected in its ability to improve the overall stability of the ecosystem and its resilience to external disturbances. Higher connectivity facilitates the migration and gene exchange of biological populations, thereby maintaining biodiversity and ecosystem services [58],[59]. Most of the other regions were negatively correlated. One possible reason is that higher cohesion leads to a smaller number of species within the region and a decline in ecosystem service functions. As a result, the ESI was also reduced [60].To further verify these notions, we analyzed the correlation between the PD, SHDI, LSI, and ESI (**Fig. 9b,c,d**). These three indices were found to have large positive correlations with the ESI in the middle reaches of the YRB region. This demonstrated that the more complex and species-rich the landscape in the region, the greater the contribution to the ESI. Increased PD and SHDI indices imply higher biodiversity, which is essential for the provision of ecosystem services. Ecosystems with high biodiversity are typically more productive, recycle nutrients and water more efficiently, and enhance ecosystem resilience to environmental change, thereby increasing ESI [61],[62]. The LSI reflects the complexity of landscape boundaries, with higher LSI indicating increased landscape heterogeneity. Increased landscape heterogeneity can provide more ecological niches and habitat types, promote species diversity and diversification of ecosystem functions, and enhance ecosystem resilience to disturbances and self-recovery [63],[64]. Landscape complexity and ESI showed a large negative correlation in the upstream eastern region of Qinghai Province. This showed that spatial tightness and connectivity had a promoting effect on ESI in this region. The response of the ESI to the landscape index was not significant in the Ordos Plateau, the Hetao Plain, the Ningxia Plain, and the hinterland of the Loess Plateau. This was related to the low complexity and diversity of the region's ecological landscape. In this case, even if there was some environmental change or disturbance, the response of landscape indices to ESI may not

be significant due to species homogeneity [65]. In summary, we found that the relationship between landscape indices and ESI is manifested by influencing ecosystem stability, biodiversity, resilience to disturbance, and the provision of ecosystem services. Different regions of the YRB respond differently to landscape complexity, and site-specific planning and design should be adopted in future development. The ecological safety level of the YRB can be effectively enhanced by optimizing the landscape configuration.

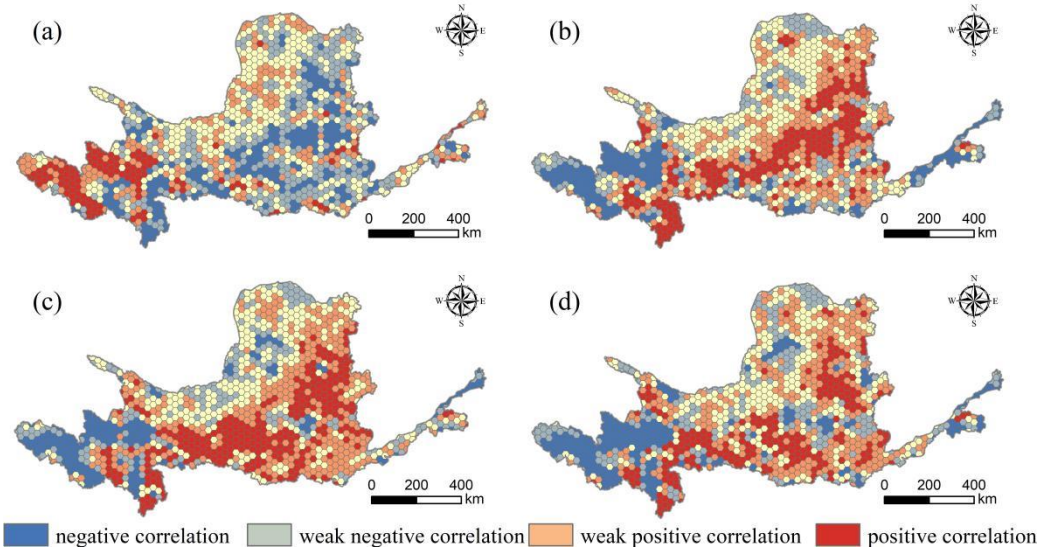

Fig. 9. Spatial distribution of correlation coefficients between ESI and landscape indices(a) Cohesion; (b)PD; (c)SHDI; (d)LSI

C. Future trends of the YRB's ESI

1) Characteristics of future temporal changes in ESI in the YRB

In this study, we used the constructed LSTM to predict the spatial pattern of the YRB in 2021-2030, and calculate the annual average of ESI in the next 10 years. By linearly fitting the trend of ESI, the interannual variation characteristics of ESI are described, as shown in **Fig. 10**. Overall, the ESI of the YRB will show a fluctuating upward trend, and the rising rate is 0.0014/a, which is less than the historical data. The highest and lowest values of ESI will be in 2029 and 2024, with values of 0.51 and 0.48, respectively. In summary, YRB's ESI will show an upward trend in the next 10 years, but the rate of increase will be smaller than that in the previous 21 years.

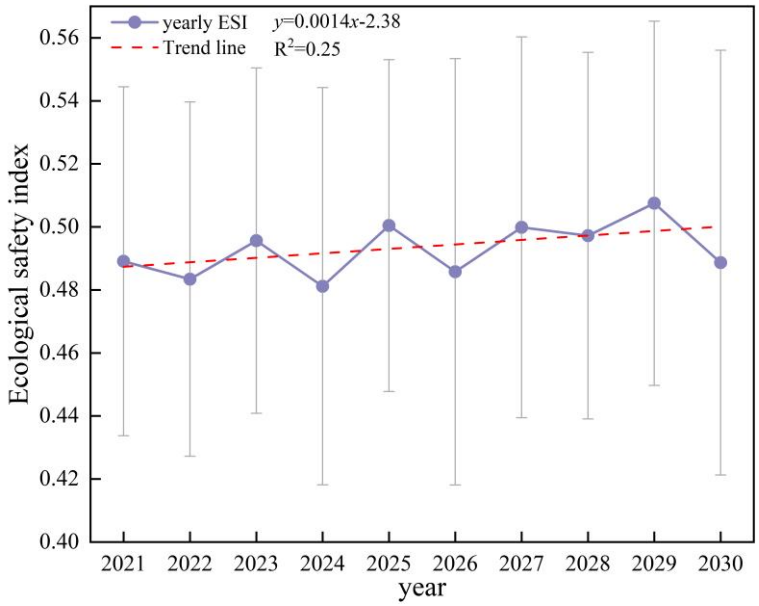

Fig. 10. Change in ESI future annual averages

2) Characteristics of future spatial changes in the YRB's ESI

We used the prediction model to obtain the ESI spatial distribution results of the YRB over the next 10 years, as

shown in **Fig. 11**. The spatial distribution of the predicted results shows an increase in hazardous areas in the downstream basins of Jinan and Tai' an in the future. The distribution of other regions will be roughly the same as the historical data.

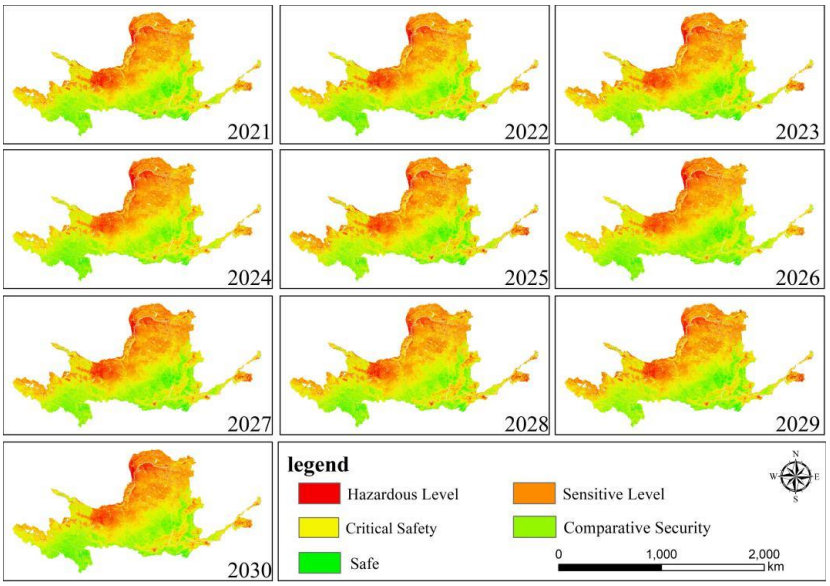

Fig. 11.Future spatial distribution of ESI

In this study, the TS trend analysis and the MK test were performed on the forecast results of ESI, and the results are shown in **Fig. 12a**. Most of YRB's ESI will show an upward trend in the next 10 years.

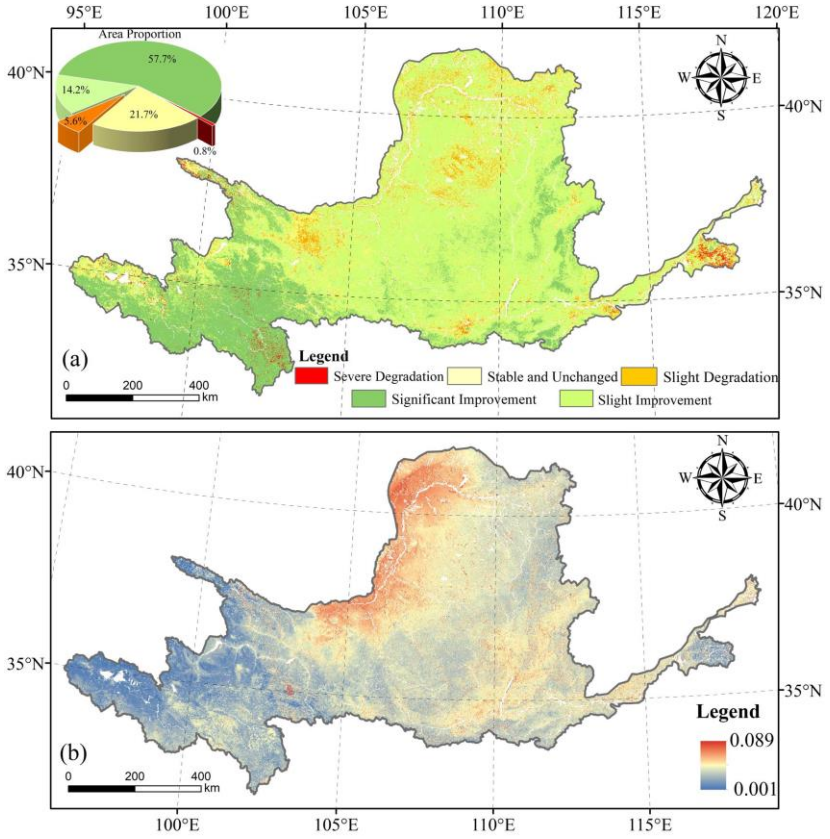

Fig. 12.(a) Spatial distribution of ESI trends over the next 10 years; (b) Spatial distribution of ESI variance indices over the next 10 years

However, compared with the past 21 years, the area with significant growth will decrease, and the area with slight growth will increase. Areas with severe degradation and slight degradation will increase. The areas that will experience an increase will be mainly distributed in the southwest and central part of Gansu Province, Hetao Plain, Ordos Plateau and Jinan, Tai ‘an and other regions in the central part of Shandong Province. Other degraded areas are consistent with historical areas. From the CV of the ESI, the changes in the northwest region of the YRB remained unstable(**Fig. 12b**). However, these regions in western Sichuan Province and the Loess Plateau will be more stable in terms of ESI than before. In summary, the upward trend of most areas of the YRB in the next 10 years will decrease compared to the previous years, and the proportion of degraded areas will increase. YRB’s ESI will be more stable in the future, but changes in the desert regions of the northwest will remain volatile.

V. DISCUSSION

A. ESI accuracy analysis

Based on the important role of vegetation in the ecosystem of the YRB, this study constructed a comprehensive, multi-dimensional ecological safety evaluation system, “vigor-pressure-state-response,” for the study area of the YRB, with vegetation as the core of “vigor”. The logical relationships of the constructed index system were then verified using SEM. The final fitted SEM model is shown in **Fig. 13**. The goodness-of-fit indices were: CFI = 0.98, RMSEA < 0.001, SRME < 0.001, indicating a good model fit. According to the results, pressure had a significant negative impact on vigor and state. Vigor had a significant positive effect on state and response, and had the most significant effect on response. Pressure had a slight positive impact on response because it included economic aspects. The state of the region had a slight negative impact on the response due to the constraints of the geographical environment. Thus, we can conclude that the final model-fitting results coincide with the logical preconception of constructing the index, indicating that the constructed comprehensive multiscale evaluation system is reasonable.

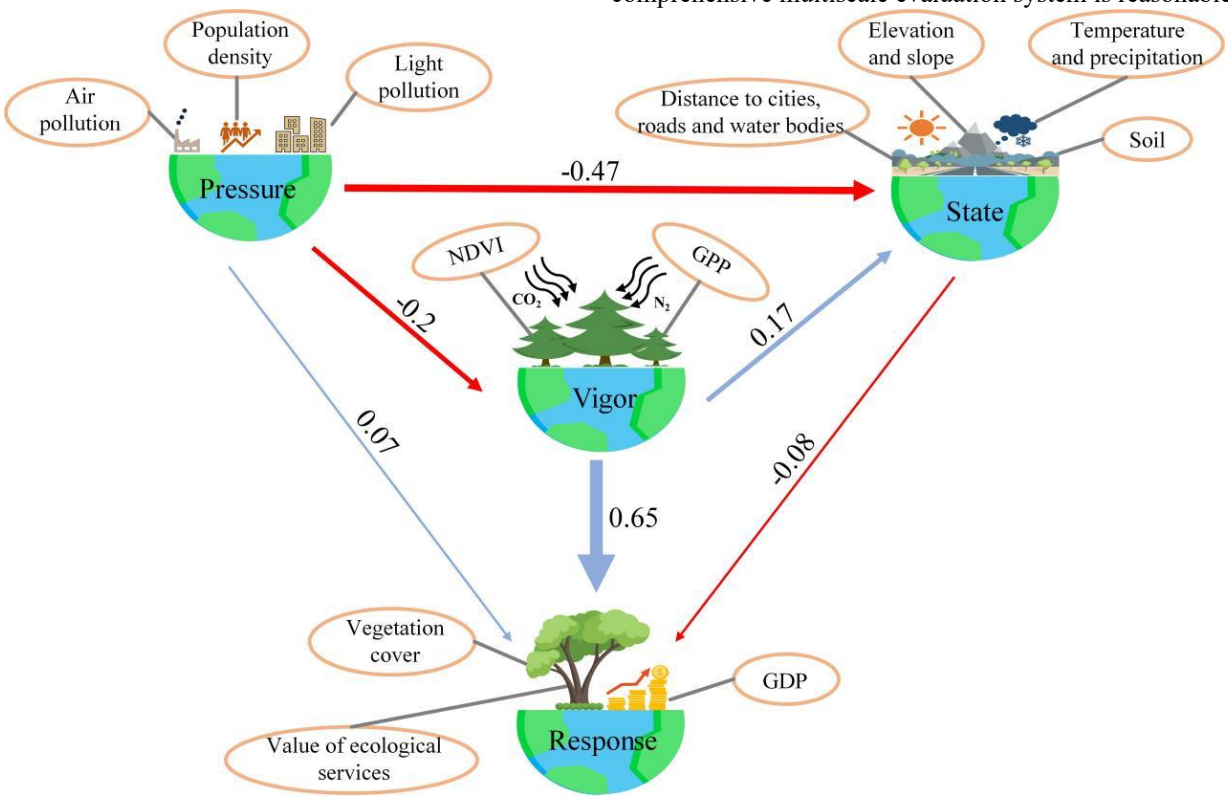

Fig.13. Relationship between the effects of different factors

The eco-environmental quality index (EQI) is a comprehensive evaluation indicator. It consists of a combination of atmospheric, water, surface temperature, and biodiversity data to assess the health of the ecosystem [66]. A higher EQI usually means better environmental quality, relatively stable ecosystems, and higher species richness. These are essential for ecological safety. Conversely, if the EQI is low, the ecosystem will face threats that could lead to ecological disasters, posing significant risks to humans and other organisms. Thus, there is a close and mutually reinforcing relationship between EQI and ESI [67]. To verify the accuracy of the constructed ESI, we calculated a linear

regression of the EQI on the ESI for the years 2000-2020 (**Fig. 14**). The R^2 was calculated to be 0.68, indicating a strong correlation between them. This verifies that the ESI we constructed is plausible.

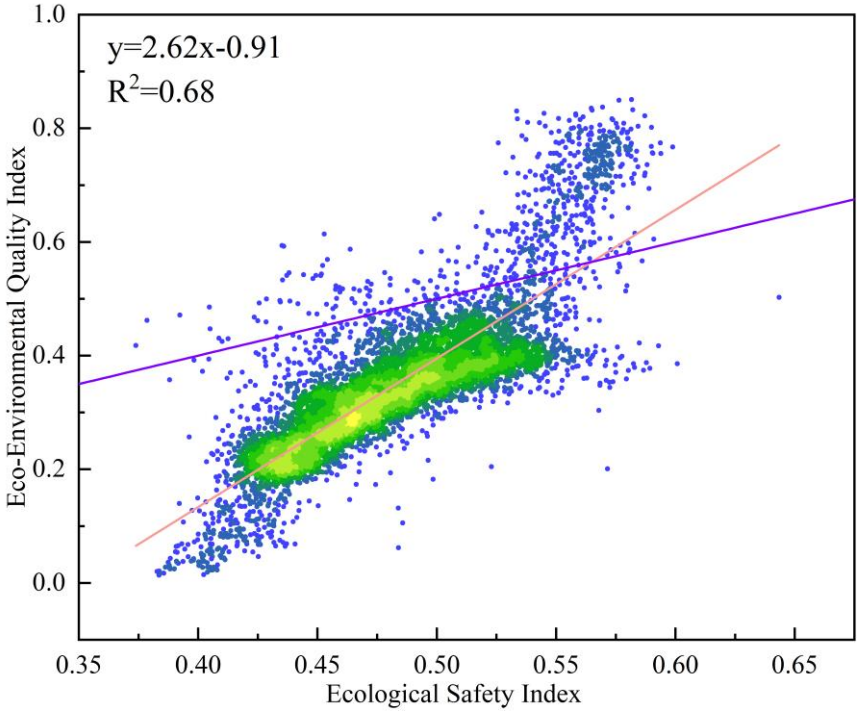

Fig. 14. Scatterplot of ESI vs EQI correlation

B. Analysis of spatiotemporal changes in the ESI

The ESI of the YRB showed an upward trend year by year, reflecting the initial results of ecological protection and management measures in recent years [68]. However, the volatility of ESI was large, indicating that the improvement process of ecological safety was unstable and vulnerable to many factors. Spatially, the ESI showed obvious regional differences. The risk level and sensitive level areas of the northwest desert arid area and some urban areas were concentrated. This reflects differences in ecological pressure and the intensity of human activities in different regions. From the perspective of spatial change trends, the ESI in the arid area of northwest China has greatly improved. This may be due to ecological restoration projects and reduced human activity interventions in recent years [69]. In rapidly developing urban areas, due to high-intensity industrialization and urbanization, the pressure on the ecological environment has increased, resulting in a decline in the ESI. The prediction showed that the ESI of the YRB will continue to improve in the next 10 years, but the improvement rate will decline. Especially in most areas of the middle reaches of the Loess Plateau and the upstream areas of rapid urbanization, the problem of ecological degradation will be more significant.

Based on the above results, we propose the following control strategy recommendations: First, stakeholders should strengthen the ecological restoration of the region. Ecological restoration projects, such as returning farmland to forest and grassland, soil, and water conservation, and ecological water network construction, should be implemented in the arid areas and severely degraded areas in the northwest to improve the self-recovery ability of the ecosystem. Strict land use planning and construction standards can then be formulated for rapid urbanization areas. Further, unreasonable industrialization and urbanization development should be restricted to reduce the negative impact on the ecological environment. Finally, an ecological safety monitoring and early warning system of the YRB should be established and improved while improving the response speed and processing capacity of ecological changes and taking timely measures to deal with possible ecological risks.

C. Predictive model performance analysis

To visually verify the reliability of the LSTM-based spatiotemporal forecasting model for extracting ESI, we performed correlation calculations on the 2000-2020 ESI and forecast data, as shown in **Fig. 15a**. The correlation coefficient was 0.94, and the two correlations were high, indicating that the experimentally trained LSTM prediction model in this study was effective. **Fig. 15b** shows the results and the difference between the true and predicted values of the annual average ESI. In general, the smaller the MAE and RMSE values of the true and predicted values, and the closer the R^2 and EVar values were to 1, the better the model predicted. The MAE and RMSE values were calculated to be 0.001 and 0.002, and the R^2 and EVar values were 0.97 and

0.98, respectively. These outcomes quantitatively illustrate that the constructed LSTM model has high accuracy and can successfully capture fluctuations in ESI data.

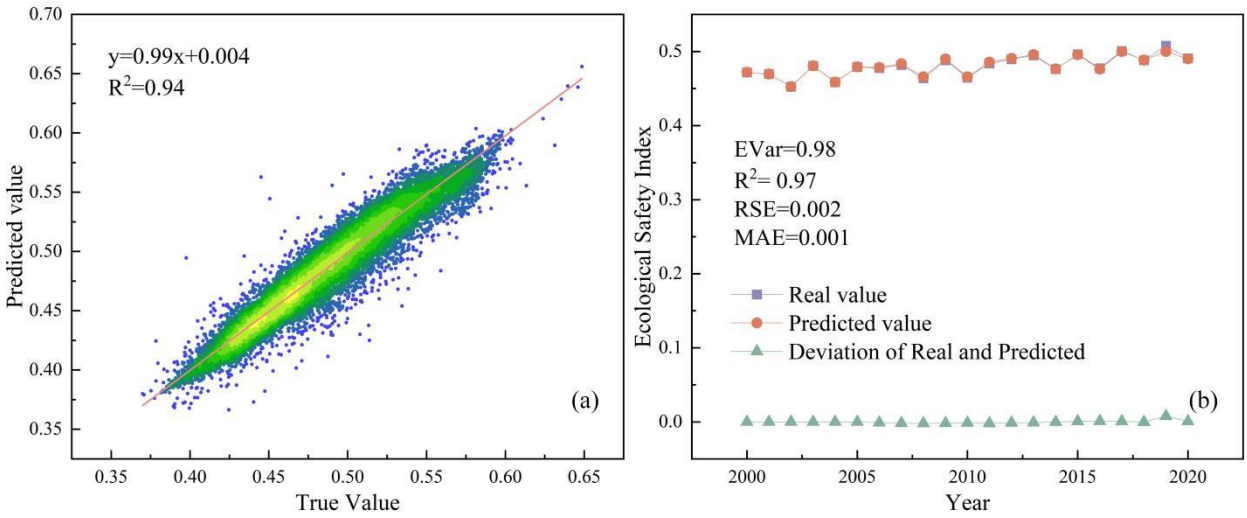

Fig. 15. (a) Scatterplot of the correlation between the true and predicted ESI values for the years 2000-2020; (b) Deviation values of the true and predicted ESI values for the years 2000-2020

D.Innovation and prospects

In this study, we improved the ecological safety evaluation model based on existing studies to better adapt it to the ecological characteristics of the YRB. We also validated the logical soundness and empirically tested the improved evaluation model. The innovations of the article are compared in detail with the differences of previous studies in **Table 5**.

Table 5

Research Comparison

Difference	Previous studies	This study	Strengths of this study
Construction of evaluation model	Ecological safety evaluation model was constructed based on socio-environmental management[18].	Ecological safety evaluation model is constructed based on vegetation change characteristics.	Good adaptability and flexibility to track ecosystem changes using vegetation sensitivity, thus providing more timely feedback and early warning.
Positive and negative judgement	Based on the subjective experience, they assessed the positive and negative effects of different influencing factors on the ecological safety of the whole study area [71].	Based on the existing response mechanism of vegetation change in the YRB, it assessed the positive and negative effects of different influencing factors on ecological safety [33],[70].	Avoids the error of determining the positive and negative effects of ecological safety indicators due to human subjective factors, making the determination more objective.
Spatiotemporal scales of the ESI	The temporal and spatial changes of ecological safety were studied based on the county spatial scale and the intermittent time scale[38].	Long time series analysis of ecological safety in the region is carried out based on pixel scale.	Provides a more detailed spatial and temporal resolution, which can more accurately identify ecologically fragile areas, ecological degradation phenomena, and potential threats to ecological safety, thus providing a more precise evaluation of the ecological safety status.
Evaluation model reasonableness	The logic of the evaluation model and the accuracy of the ESI were not tested[72],[73].	The logical relationship of the index system is verified by SEM. The accuracy of the ESI is verified using the EQI.	The ecological safety evaluation model is more convincing and improves the accuracy of the model.

The ecological safety of the YRB covers a wide range of aspects. It includes climate change, environmental pollution, changes in land use types, and the expansion of urban agglomerations. All of these have implications for ecological

safety. Future studies should consider adding more factors that have an impact on ecological safety to improve the ESI and reflect the real situation of ecological safety in the YRB more comprehensively and accurately. Further, using remote sensing data, such as NDVI, introduces their inherent uncertainty, which has an impact on the construction of the index. These uncertainties come from many aspects, including sensor errors, atmospheric effects, data processing methods, and differences in model parameters. Therefore, in the process of data processing, the influence of these uncertain factors on the results should be taken into account, and corresponding error analyses and controls should be carried out. In addition, this study analyzed only the changes in ESI and did not explore the characteristics of the changes in its internal criterion layers (“vigor-pressure-state-response”). Therefore, future studies should pay attention to the changes in intrinsic factors to gain a deeper understanding of the internal causes of ESI.

VI. CONCLUSION

Based on the“vigor-pressure-state-response”model, this study constructed the ESI of the YRB from 2000 to 2020. The change characteristics of the ESI were then analyzed, and the relationship between the ESI and the landscape index was explored. The LSTM model was used to predict the ecological safety changes in the YRB over the next 10 years. The ESI of the YRB showed a fluctuating upward trend at a rate of 0.0016/a during 2000-2020. The spatial distribution of ESI showed significant differences. The spatial distribution showed significant positive agglomeration characteristics, dominated by the spatial characteristics of high-high agglomeration and low-low agglomeration. The ESI for the desert arid regions in the upper reaches and some urban areas in the middle and lower reaches were hazardous and sensitive. The spatial change trend of the ESI showed a significant increase in most of the regions, except for the northwestern region of the YRB, which showed a slight improvement. A small number of degraded areas were mainly urban areas with high levels of human activity. The stability of the ESI was weaker in regions with high desertification, developed animal husbandry and high ESI values on the Loess Plateau. Combined with the landscape index study, we found that the ESI in most of the middle reaches of the YRB was positively correlated with the complexity of the landscape, while some of the upstream and downstream areas showed non-significant or negative correlations. The rate of increase in YRB’s ESI will slow down in the next 10 years, and more ecological hazard class areas will appear in the upstream zone. In terms of spatial trends, the proportion of degraded areas will increase, while the proportion of areas with significant growth will decrease. The stability of future ESI changes will improve, but changes in the northwest desert region will remain volatile.

ACKNOWLEDGEMNT

Acknowledgement for the data support from "National Earth System Science Data Center, National Science & Technology Infrastructure of China. (http://www.geodata.cn).In addition, we would like to thank Prof. Jinfeng Wang for the free software GeoDetector.

REFERENCES

[1] M. Zhang *et al.*, “Ecological security evaluation and ecological regulation approach of East-Liao River basin based on ecological function area,” *Ecol Indic*, vol. 132, Dec. 2021, doi: 10.1016/j.ecolind.2021.108255.

[2] Yun Chen, Jinliang Wang.,“Ecological safety early-warning in central Yunnan Province, China, based on the gray model,"Ecol Indic, vol. 111, Dec. 2021, doi: 10.1016/j.ecolind.2019.106000.

[3] Hao-jie Xu, Chuan-yan Zhao, Sheng-yun Chen, et al., “ Spatial relationships among regulating ecosystem services in mountainous regions: Nonlinear and elevation-dependent, " Journal of Cleaner Production,vol 380,2022, doi:10.1016/j.jclepro.2022.135050.

[4] Mingxi Zhang, Yongbin Bao, Jie Xu.,“Ecological safety early-warning in central Yunnan Province, China, based on the gray model,"Ecol Indic, vol. 111, 2021, doi: 10.1016/j.ecolind.2021.108255.

[5] Shu-yao Shan, Hao-jie Xu, Xiao-lian Qi, et al.,“Evaluation and prediction of ecological carrying capacity in the Qilian Mountain National Park, China, " Journal of Environmental Management,vol 339,2023,doi:10.1016/j.jenvman.2023.117856.

[6] S. Tian et al., “Urban ecological security assessment and path regulation for ecological protection - A case study of Shenzhen, China,” Ecol Indic, vol. 145, Dec. 2022, doi: 10.1016/j.ecolind.2022.109717.

[7] S. H. Sadeghi *et al.*, “Watershed health and ecological security zoning throughout Iran,” *Science of the Total Environment*, vol. 905, Dec. 2023, doi: 10.1016/j.scitotenv.2023.167123.

[8] M. Jiao *et al.*, “Construction and influencing factors of an early warning system for marine ranching ecological security: Experience from China’s coastal areas,” *J Environ Manage*, vol. 335, Jun. 2023, doi: 10.1016/j.jenvman.2023.117515.

[9] M. Qiu, Q. Zuo, Q. Wu, Z. Yang, and J. Zhang, “Water ecological security assessment and spatial autocorrelation analysis of prefectural regions involved in the Yellow River Basin,” *Sci Rep*, vol. 12, no. 1, Dec. 2022, doi: 10.1038/s41598-022-07656-9.

[10] T. Li *et al.*, “Identification of Degradation Areas of Ecological Environment and Degradation Intensity Assessment in the Yellow River Basin,” *Front Earth Sci (Lausanne)*, vol. 10, Jul. 2022, doi: 10.3389/feart.2022.922013.

[11] Jian Liu, Lihong Wei, Zhaopei Zheng, et al.,“Vegetation cover change and its response to climate extremes in the Yellow River Basin," Science of The Total Environment, vol

905,2023,doi:10.1016/j.scitotenv.2023.167366.

[12] Menghao Yang, Xiaodong Gao, Kadambot H.M. , et al.,"Spatiotemporal exploration of ecosystem service, urbanization, and their interactive coercing relationship in the Yellow River Basin over the past 40 years," Science of The Total Environment, vol 858, 2023, doi:10.1016/j.scitotenv.2022.159757.

[13] T. Li *et al.*, "Ecological degradation in the Inner Mongolia reach of the Yellow River Basin, China: Spatiotemporal patterns and driving factors," *Ecol Indic*, vol. 154, Oct. 2023, doi: 10.1016/j.ecolind.2023.110498.

[14] H. Li, Y. He, L. Zhang, S. Cao, and Q. Sun, "Spatiotemporal changes of Gross Primary Production in the Yellow River Basin of China under the influence of climate-driven and human-activity," *Glob Ecol Conserv*, vol. 46, Oct. 2023, doi: 10.1016/j.gecco.2023.e02550.

[15] L. Du, C. Dong, X. Kang, X. Qian, and L. Gu, "Spatiotemporal evolution of land cover changes and landscape ecological risk assessment in the Yellow River Basin, 2015–2020," *J Environ Manage*, vol. 332, Apr. 2023, doi: 10.1016/j.jenvman.2022.117149.

[16] Y. Zhang *et al.*, "Identifying ecological security patterns based on the supply, demand and sensitivity of ecosystem service: A case study in the Yellow River Basin, China," *J Environ Manage*, vol. 315, Aug. 2022, doi: 10.1016/j.jenvman.2022.115158.

[17] Y. Li *et al.*, "The role of land use change in affecting ecosystem services and the ecological security pattern of the Hexi Regions, Northwest China," *Science of the Total Environment*, vol. 855, Jan. 2023, doi: 10.1016/j.scitotenv.2022.158940.

[18] Yuxin Tian , Meirong Tian, Chaoyang Feng, et al.,"Study on Ecological Security Evaluation Index System of the Yellow River Basin," E3S Web of Conferences, vol 393, May. 2023, doi: 10.1051/e3sconf/202339302018.

[19] Guolong Zhang, Jianping Huang, et al.,"The evolution of ecological Security and its drivers in the Yellow River Basin," Environmental Science and Pollution Research, vol 30, 2023, doi:10.1007/s11356-023-25667-5.

[20] G. Geng, R. Yang, and L. Liu, "Downscaled solar-induced chlorophyll fluorescence has great potential for monitoring the response of vegetation to drought in the Yellow River Basin, China: Insights from an extreme event," Ecol Indic, vol. 138, May 2022, doi: 10.1016/j.ecolind.2022.108801.

[21]M. Zhu et al., "Response of vegetation carbon sequestration potential to the effectiveness of vegetation restoration in karst ecologically fragile areas in Guizhou, southwest China," Ecol Indic, vol. 158, Jan. 2024, doi: 10.1016/j.ecolind.2023.111495.

[22]Y. Bai, M. Liu, Q. Guo, G. Wu, W. Wang, and S. Li, "Diverse responses of gross primary production and leaf area index to drought on the Mongolian Plateau," Science of the Total Environment, vol. 902, Dec. 2023, doi: 10.1016/j.scitotenv.2023.166507.

[23] S. Cao et al., "Spatiotemporal dynamics of vegetation net ecosystem productivity and its response to drought in Northwest China," GIsci Remote Sens, vol. 60, no. 1, 2023, doi: 10.1080/15481603.2023.2194597.

[24] L. Jiang, W. Liu, B. Liu, Y. Yuan, and A. Bao, "Monitoring vegetation sensitivity to drought events in China," Science of the Total Environment, vol. 893, Oct. 2023, doi: 10.1016/j.scitotenv.2023.164917.

[25] He, Y., Yan, H., Ma, L. et al."Spatiotemporal dynamics of the vegetation in Ningxia, China using MODIS imagery," Front. Earth Sci.vol. 14, pp.221–235,Oct.2020. doi:10.1007/s11707-019-0767-7

[26] Yunrui Ma, Qingyu Guan, Yunfan Sun, Jun Zhang, Liqin Yang, Enqi Yang, Huichun Li, Qinqin Du."Three-dimensional dynamic characteristics of vegetation and its response to climatic factors in the Qilian Mountains,"CATENA.vol. 208, Jan.2022. doi:10.1016/j.catena.2021.105694.

[27] Y. Bai, N. Bhattarai, K. Mallick, S. Zhang, T. Hu, and J. Zhang, "Thermally derived evapotranspiration from the Surface Temperature Initiated Closure (STIC) model improves cropland GPP estimates under dry conditions," Remote Sens Environ, vol. 271, Mar. 2022, doi: 10.1016/j.rse.2022.112901.

[28] H. Hou et al., "Future Land Use/Land Cover Change Has Nontrivial and Potentially Dominant Impact on Global Gross Primary Productivity," Earths Future, vol. 10, no. 9, Sep. 2022, doi: 10.1029/2021EF002628.

[29] Q. Tang, L. Hua, Y. Cao, L. Jiang, and C. Cai, "Human activities are the key driver of water erosion changes in northeastern China," Land Degrad Dev, Jan. 2023, doi: 10.1002/ldr.4897.

[30] Y. Zhao et al., "Effects of human activity intensity on habitat quality based on nighttime light remote sensing: A case study of Northern Shaanxi, China," Science of the Total Environment, vol. 851, Dec. 2022, doi: 10.1016/j.scitotenv.2022.158037.

[31] Y. Guan, Y. Xiao, B. Rong, L. Kang, N. Zhang, and C. Chu, "Heterogeneity and typology of the city-level synergy between CO2 emission, PM2.5, and ozone pollution in China," J Clean Prod, vol. 405, Jun. 2023, doi: 10.1016/j.jclepro.2023.136871.

[32] Z. Yu et al., "Environmental surveillance in Jinan city of East China (2014–2022) reveals improved air quality but remained health risks attributable to PM2.5-bound metal contaminants," Environmental Pollution, p. 123275, Feb. 2023, doi: 10.1016/j.envpol.2023.123275.

[33]Xiao.Wei,L. Zhang,Y. He,et al,"Spatial and temporal variation characteristics of different vegetation types in the Yellow River Basin and their influencing factors from 2000 to 2020,"Remote Sensing for Natural Resources,Aug.2023,doi:10.6046/zrzyyg.2023138

[34] Y. Ding et al., "Spatiotemporal evolution of agricultural drought and its attribution under different climate zones and vegetation types in the Yellow River Basin of China," Science of the Total Environment, vol. 914, Mar. 2024, doi: 10.1016/j.scitotenv.2023.169687.

[35] Ning L ,"Study on the Influence of Economic Growth on Ecological Environment Quality in China," Chang'an University,2022.

[36] C. Liu et al., "Detection of vegetation coverage changes in the Yellow River Basin from 2003 to 2020," Ecol Indic, vol. 138, May 2022, doi: 10.1016/j.ecolind.2022.108818.

[37] Qin M X, Yang C C, Xu L S, et al."Analysis of the spatiotemporal evolution of the coordinated development of ecosystem service value and economy in the Yellow River Basin," *Journal of Earth Environment*, vol. 13(4) ,pp: 491–505 Aug.2022,doi:10.7515/JEE222022

[38] S. Lu, X. Tang, X. Guan, F. Qin, X. Liu, and D. Zhang, "The assessment of forest ecological security and its determining indicators: A case study of the Yangtze River Economic Belt in China," *J Environ Manage*, vol. 258, Mar. 2020, doi:10.1016/j.jenvman.2019.110048

[39] Gao, B., He, Y., Chen, X., Zheng, X., Zhang, L., Zhang, Q., & Lu, J, " Landslide risk evaluation in Shenzhen based on stacking ensemble learning and InSAR,"*IEEE Journal of Selected Topics in Applied Earth Observations and Remote Sensing*, vol.16,pp:1–17.

[40] K. Sun et al, "Ecological security evaluation and early warning in the water source area of the Middle Route of South-to-North Water Diversion Project," Science of the Total Environment, vol. 868, Apr. 2023, doi: 10.1016/j.scitotenv.2023.161561.

[41] WANG Yishan, ZHANG Fei, CHEN Rui,et al, "Comprehensive ecological security assessment: A case study of Urumqi City,"*ARID LAND GEOGRAPHY*, vol. 44. Mar.2021,pp:427-440, doi:10.12118/j.issn.1000－6060. 2021. 02. 14.

[42] J L Liang,W X Chen,J F Li ,et al, "Spatiotemporal patterns of landscape fragmentation and causes in the Yellow River Basin,"*Acta Ecological Sinica* ,vol.42, Mar.2022, pp:1993-2009,doi: 10.5846/stxb202102100426

[43] H. Zeng, C. Zhao, Y. Wang,et al, "Landscape pattern evolution and its influencing factors of alpine wetland in Yanchi Bay,"*ARID ZONE RESEARCH*,vol.38Nov.2021,pp:1771-1781,doi:10.13866/j.azr.2021.06.29

[44] S G Cao, Shuang C, "Analysis of quality evolution important ecological function areas and implementation effects of the ecological redline in Jiangsu Province China,"*Acta Ecological Sinica*,vol.43,Nov.2023, doi:10.20103/j.stxb.202208212398

[45] M. Hu, Z. Li, M. Yuan, C. Fan, and B. Xia, "Spatial differentiation of ecological security and differentiated management of ecological conservation in the Pearl River Delta, China," Ecol Indic, vol. 104, pp. 439–448, Sep. 2019, doi: 10.1016/j.ecolind.2019.04.081.

[46] L. Zhang, H. Yan, Y. He, S. Yao, S. Cao, and Q. Sun, "Spatiotemporal Prediction of Alpine Vegetation Dynamic Change Based on a ConvGRU Neural Network Model: A Case Study of the Upper Heihe River Basin in Northwest China," *IEEE Journal of Selected Topics in Applied Earth Observations and Remote Sensing*, vol. 15, pp. 6957–6971, 2022, doi: 10.1109/JSTARS.2022.3200521.

[47] Q.Sun, L.Zhang,Y HE ,et al, "Spatio-temporal changes and driving force analysis of vegetation net primary productivity in Gannan Tibetan Autonomous Prefecture," Pratacultural Science, 2023, vol.40, pp: 1729-1741.doi: 10.11829/j.issn.1001-0629.2022-0204

[48] C. Hong, X. Jin, J. Ren, Z. Gu, and Y. Zhou, "Satellite data indicates multidimensional variation of agricultural production in land consolidation area," Science of the Total Environment, vol. 653, pp. 735–747, Feb. 2019, doi: 10.1016/j.scitotenv.2018.10.415.

[49] L. Zhang, H. Yan, L. Qiu, S. Cao, Y. He, and G. Pang, "Spatial and temporal analyses of vegetation changes at multiple time scales in the qilian mountains," *Remote Sens (Basel)*, vol. 13, no. 24, Dec. 2021, doi: 10.3390/rs13245046.

[50] L S. QIU,Y. HE,L. Zhang, et al.Spatiotemporal variation characteristics and influence factors of MODIS LST in Qilian Mountains.*Aridland Geography*,vol.43, pp:726-737,May.2020, doi:10．12118/j．issn．1000－6060．2020．03．19

[51] C. Li et al., "Drivers and impacts of changes in China's drylands," *Nature Reviews Earth and Environment*, vol. 2, no. 12, pp. 858–873, Dec. 01, 2021. doi: 10.1038/s43017-021-00226-z.

[52] T. Zhang, Y. Chen, and S. Ali, "Abiotic stress and human activities reduce plant diversity in desert riparian forests," *Ecol Indic*, vol. 152, Aug. 2023, doi: 10.1016/j.ecolind.2023.110340.

[53] Y. Guo et al., "LSTM time series NDVI prediction method incorporating climate elements: A case study of Yellow River Basin, China," J Hydrol (Amst), vol. 629, p. 130518, Feb. 2024, doi: 10.1016/j.jhydrol.2023.130518.

[54]Y. Fang et al., "The Displacement Analysis and Prediction of a Creeping Ancient Landslide at Suoertou, Zhouqu County, China," IEEE J Sel Top Appl Earth Obs Remote Sens, 2024, doi: 10.1109/JSTARS.2024.3357520.

[55] S. Cao et al., "Spatiotemporal characteristics of drought and its impact on vegetation in the vegetation region of Northwest China," Ecol Indic, vol. 133, Dec. 2021, doi: 10.1016/j.ecolind.2021.108420.

[56] J. Peng, Y. Liu, T. Li, and J. Wu, "Regional ecosystem health response to rural land use change: A case study in Lijiang City, China," Ecol Indic, vol. 72, pp. 399–410, Jan. 2017, doi: 10.1016/j.ecolind.2016.08.024.

[57]B. Wang, M. Ding, S. Li, L. Liu, and J. Ai, "Assessment of landscape ecological risk for a cross-border basin: A case study of the Koshi River Basin, central Himalayas," Ecol Indic, vol. 117, Oct. 2020, doi: 10.1016/j.ecolind.2020.106621.

[58]Min Li, Guangjie Luo, Yangbing Li,et al.,"Effects of landscape patterns and their changes on ecosystem health under different topographic gradients: A case study of the Miaoling Mountains in southern China," Ecological Indicators, vol 154, 2023, doi:10.1016/j.ecolind.2023.110796.

[59] L. Zheng, Y. Wang, and J. Li, "Quantifying the spatial impact of landscape fragmentation on habitat quality: A multi-temporal dimensional comparison between the Yangtze River Economic Belt and Yellow River Basin of China," Land use policy, vol. 125, Feb. 2023, doi: 10.1016/j.landusepol.2022.106463.

[60]S. Li et al., "Optimization of landscape pattern in China Luojiang Xiaoxi basin based on landscape ecological risk assessment," Ecol Indic, vol. 146, Feb. 2023, doi: 10.1016/j.ecolind.2023.109887.

[61]]P. Ran, S. Hu, A. E. Frazier, S. Yang, X. Song, and S. Qu, "The dynamic relationships between landscape structure and ecosystem services: An empirical analysis from the Wuhan metropolitan area, China, " J Environ Manage, vol. 325, Jan. 2023, doi: 10.1016/j.jenvman.2022.116575.

[62]H. Zhang, L. Xue, G. Wei, Z. Dong, and X. Meng, "Assessing vegetation dynamics and landscape ecological risk on the mainstream of Tarim River, China," Water (Switzerland), vol. 12, no. 8, Aug. 2020, doi: 10.3390/W12082156.

[63]Y. Han, D. Chang, X. zhi Xiang, and J. lei Wang, "Can ecological landscape pattern influence dry-wet dynamics? A national scale assessment in China from 1980 to 2018," Science of the Total Environment, vol. 823, Jun. 2022, doi: 10.1016/j.scitotenv.2022.153587.

[64]W. Li, Y. Wang, S. Xie, R. Sun, and X. Cheng, "Impacts of landscape multifunctionality change on landscape ecological risk in a megacity, China: A case study of Beijing," Ecol Indic, vol. 117, Oct. 2020, doi: 10.1016/j.ecolind.2020.106681.

[65] L. Ma, J. Bo, X. Li, F. Fang, and W. Cheng, "Identifying key landscape pattern indices influencing the ecological security of inland river basin: The middle and lower reaches of Shule River Basin as an example," *Science of the Total Environment*, vol. 674, pp. 424–438, Jul. 2019, doi: 10.1016/j.scitotenv.2019.04.107.

[66] D. Xu et al., "Quantization of the coupling mechanism between eco-environmental quality and urbanization from multisource remote sensing data,"J Clean Prod, vol. 321, Oct. 2021, doi: 10.1016/j.jclepro.2021.128948.

[67] L. Yang, S. Pan, W. Chen, J. Zeng, H. Xu, and T. Gu, "Spatially non-stationary response of habitat quality to land use activities in World's protected areas over 20 years," *J Clean Prod*, vol. 419, Sep. 2023, doi: 10.1016/j.jclepro.2023.138245.

[68] L. Fang et al., "Identifying the impacts of natural and human factors on ecosystem service in the Yangtze and Yellow River Basins," J Clean Prod, vol. 314, Sep. 2021, doi: 10.1016/j.jclepro.2021.127995.

[69]Y. Gao et al., "Identifying the spatio-temporal pattern of drought characteristics and its constraint factors in the Yellow River Basin," Ecol Indic, vol. 154, Oct. 2023, doi: 10.1016/j.ecolind.2023.110753.

[70]M. A. Akram et al., "Variations and driving factors of leaf functional traits in the dominant desert plant species along an environmental gradient in the drylands of China," Science of the Total Environment, vol. 897, Nov. 2023, doi: 10.1016/j.scitotenv.2023.165394.

[71] Luo HP, Li ZY, Wang JC.,"Agricultural ecological security evaluation and obstacle factor diagnosis of main grain producing areas in China based on PSR model, " J. Stat. Inform, vol37, 2022. doi:1001-4829(2022) 10-2436-09.

[72]S. Lu et al., "Spatiotemporal differences in forest ecological security warning values in Beijing: Using an integrated evaluation index system and system dynamics model," Ecol Indic, vol. 104, pp. 549–558, Sep. 2019, doi: 10.1016/j.ecolind.2019.05.015.

[73]Z. rong Ou, Q. ke Zhu, and Y. yu Sun, "Regional ecological security and diagnosis of obstacle factors in underdeveloped regions: a case study in Yunnan Province, China," J Mt Sci, vol. 14, no. 5, pp. 870–884, May 2017, doi: 10.1007/s11629-016-4199-5.